Transport of fast excited ions through thin solids probed by X-ray spectroscopy

2015 J. Phys.: Conf. Ser. 629 012002

(http://iopscience.iop.org/1742-6596/629/1/012002)

Journal of Physics: Conference Series **629** (2015) 012002 doi:10.1088/1742-6596/629/1/012002

Transport of fast excited ions through thin solids probed by X-ray spectroscopy

E Lamour[1,2], J-P Rozet[1,2], D Vernhet[1,2], B Gervais[1], J-P Grandin[1], D Lelievre[1], J-M Ramillon[1] and H Rothard[1]

[1] CNRS, UMR 7588, Institut des NanoSciences de Paris (INSP), F-75005 Paris, France

[2] Sorbonne Universités, UPMC Univ. Paris 06, UMR 7588, INSP, F-75005 Paris, France

[3] Centre de Recherche sur les Ions, les Matériaux et la Photonique (CIMAP), UMR 6252 (CEA/CNRS/ENSICAEN/UCBN), F-14070 Caen Cedex 05

E-mail: emily.lamour@upmc.fr

Abstract. Over more than a decade, experimental studies of the production and transport of projectile excited states in thin solid targets have been performed at GANIL for Ar^{17+} and Kr^{35+} in the so-called high velocity domain. A range of target thicknesses from single collision condition to equilibrium has been investigated. X-ray spectroscopy techniques have allowed us to determine *absolute* $n\ell$ populations of core and Rydberg projectile states, as well as the relative population of fine structure substates ($n\ell_j$). In parallel, theoretical simulations to treat on the same footing all the competing processes, i.e., collisions, radiative decay and dynamical screening due to the wake field, have been developed. Methods based on either master equations or Monte Carlo approaches have allowed us to reach an unprecedented precision in the description of the ion transport in matter in the perturbative regime. In particular, a first direct measurement of the wake field usually extracted from ion stopping power has been performed.

1. Introduction

Fast Highly Charged Ions (HCIs) going through matter induce material modifications like, for instance, the formation of tracks in insulating materials, and in turn, their stopping power, charge state and excited states depend on the material encountered. Two different representations have been used to describe the interaction between fast highly charged ions and solid targets. They correspond to different approaches for calculating, for instance, the slowing down of a projectile through materials. In the first picture, one assumes that the ion-solid interaction is the result of a series of binary collisions with the target electrons, and *ion-atom cross sections* correspond to the data base of the *collisional* calculations. For the ion stopping power, this approach is directly related to the Bethe theory [1] taking into account explicitly the distortion of target wave-functions (more details can be found in [2] and [3]). In the other picture, closer in spirit to the *dielectric* theory first proposed by Bohr [4], the target electrons are considered to *respond collectively* to the passage of the projectile. The HCIs induce a polarization of the medium described as a wake of electronic density fluctuation trailing the ion, the so-called *wake field*. The gradient of the wake potential leads to the establishment of an electric field, and its local value at the projectile can be used to calculate the stopping power [5-7].

Both types of calculations appear to achieve good agreement with stopping power measurements, despite a rather different physical picture for the behavior of the target electrons.
The purpose of our work shortly presented here, was to evaluate the role played by target electrons in these two pictures and to define eventually the validity limits and the applicability of corresponding models in terms of different experimental observables. It is clear that the response of the target electrons to the passage of the ion has direct consequences on the projectile ion: it is not only slowed down, but, the population of its excited states is also altered by the surrounding medium. Notably, the presence of the wake field may mix the ion excited states by Stark effect in a coherent manner while a pure collisional response of target electrons destroys any coherence. Hence, we tackled studies on the production and transport of projectile excited states by analyzing the de-excitation of these excited states to probe the solid response. The theoretical description of the ion-solid interaction has been a real challenge. Indeed, the evolution of atomic projectile states propagating through a solid originates from both dissipation and dephasing. It turned out that to address such a problem the best is to consider the ion projectile as an open quantum system (the excited ion) coupled to reservoirs representing the solid and the radiation field responsible for photon emission. We developed several complementary and overlapping types of theoretical methods: a classical simulation based on a stochastic approach of the ion transport [5] and two quantum simulations implying either the resolution of the stochastic time-dependent Schrödinger equation [6, 7] or of master equations [8, 9] as "rate"-like equations.
Several experimental observables were determined for different collision systems in the perturbative regime. We remind that the perturbative regime is reached for high projectile velocities (projectile velocity much higher than the velocity of the active electron) and/or for $Z_p \gg Z_t$ (where Z_p and Z_t stand for atomic numbers for the projectile and the target, respectively). In this regime, ionization and excitation have cross sections much larger than capture. In this publication, we restrict the presentation to a selection of our results classified in order of increasing sensitivity to either the individual processes involved and/or to the dynamical screening due to the wake field. Accordingly, we first present the populations of Rydberg states, we then discuss the core $n\ell$ (with $n < 5$) states, and finally we examine the evolution of fine structure sub-state populations ($n\ell_j$ with $n = 2$ or 3 depending on the ion species). In the next section, we give the main characteristics of the experimental methods and describe the techniques applied to determine each observable. Section 3 briefly presents the theoretical treatments. Section 4 is dedicated to an overview of the results and a comparison with the simulations. Our conclusions are summarized in the last section.

2. Experiments

All the experiments have been performed with the GANIL facilities in Caen (France) using either SME (Sortie Moyenne Energie) or LISE (Ligne d'Ions Super Epluchés) experimental areas. These beam lines allow us to work with high optical quality beams from the intermediate to the high energy regime.

2.1. Collision systems

The choice of collision systems, i.e., the ion projectile, the collision velocity, the nature of the solid and its thickness was guided to highlight the various transport effects. For the $n\ell$ populations of projectile excited states, the significance of the results arises from a simplification of the problem. To provide stringent benchmarks for theory, experiments were performed with:

- the "primary" production process of the excited states well identified and the single collision condition fulfilled even for the thickest target thickness (meaning that the multiple process probability is at most a few percent); the results, selected here, concern either capture process or single excitation processes.
- the transport of the excited states –mainly due to excitation and ionization processes- investigated over a wide range of collision numbers, from single collision conditions to the equilibrium of populations.

These conditions imply to be in the perturbative regime and to study hydrogen-like excited states for which the electronic structure and the coupling between the excited states are well known. Here, we report on major results obtained for excited Kr^{35+} (33.2 or 60 MeV/u) and Ar^{17+} (13.6 MeV/u) ions

with carbon targets. Other targets have been used, like copper or aluminum [12, 10]. The target thickness ranges from 100 Å to 1 µm. As a consequence, the ion transit time inside the target is at maximum a few tens of femtoseconds. This time is long enough for the excited states evolution to be sensitive to transport effects. Indeed, the characteristic time for the establishment of the wake field (i.e., the wake period related to the plasma frequency) is less than 0.2 fs and the Stark mixing time, for the excited configurations under investigations, remains smaller than 9 fs and than 3 fs in the case of krypton and argon, respectively. Moreover, a significant Stark effect may be observed since the radiative lifetime of those excited states is larger than the Stark mixing time for $n \geq 3$ for krypton and $n \geq 2$ for argon. Finally, the mean free times of collisional processes depend on the nature of the process and decrease rapidly with the value of the principal quantum number but its contribution can be explored also with the target thickness.

2.2. Techniques

We performed X-ray spectroscopy measurements that allow determining the population of projectile excited states. The typical experimental set-up is schematically represented Figure 1. HCIs are directed onto self-supported carbon foils with measured thicknesses and purity. In some cases, gaseous targets have also been used to control the initial population produced by the primary process. Projectile X-ray emission is recorded by different detection systems depending on the observable we want to determine:

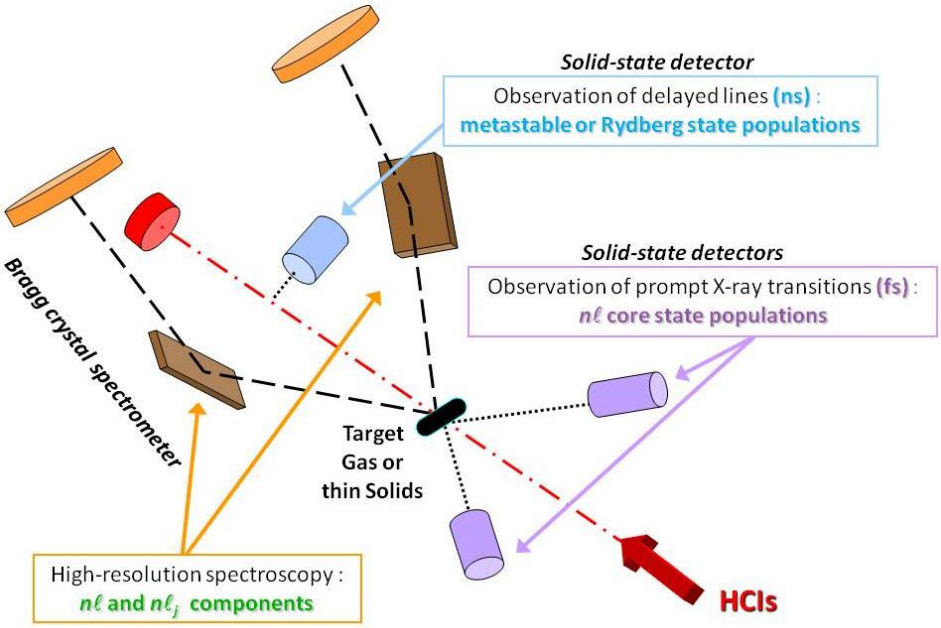

Figure 1. Schematic representation of the complete experimental set-up.

- The study of *the delayed photon emission* of short lifetime excited states (as 2p or 3p for hydrogen-like ions) is an important tool for investigating Rydberg states emerging from the solid. We have examined the delayed emission of exited Ar^{17+} ions, for each target thickness, by means of a solid-state detector placed at 90° with respect to the beam direction. Delay times, behind the target, up to 1 ns are explored with a resolution of 6×10^{-12} s. The $2s_{1/2}$ metastable state population is also determined using this system by the observation of the two-photon (2E1) transition (see figure 2).

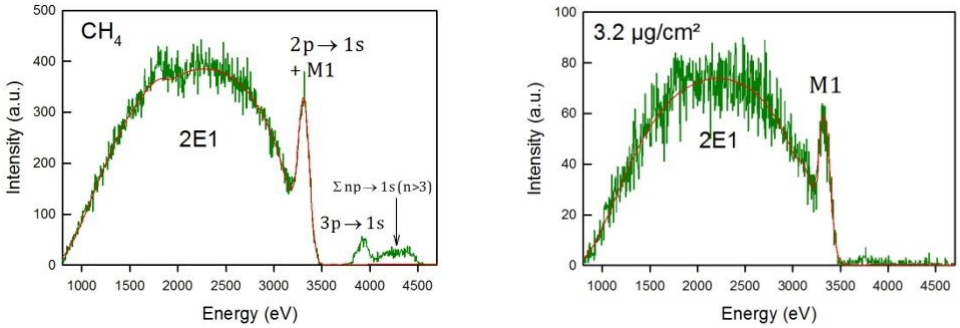

Figure 2. Spectra of the delayed X-ray transitions emitted by Ar^{17+} ions at 13.6 MeV and recorded by a solid-state detector placed at D = 127 mm behind the target for a CH_4 gaseous target and a 3.2 µg/cm² carbon foil. The 2E1 decay mode as well as the M1 one from the de-excitation of the 2s state are clearly distinguishable. Note: the photon energy is given in the projectile frame.

- *Prompt Lyman transition* intensities are measured also with solid-state detectors recording the emitted (3 to 5 keV) X-rays with the target placed at the center of the collision chamber. This allows to obtain the evolution of *np* core state populations as a function of target thickness since a very small fraction (≤ 3%) of the projectile excited states lies above $n = 10$.

For each type of emission lines – *delayed or prompt*- the energy resolution of the solid-state detectors allows us to identify Lyman lines with $n \leq 4$ (as well as the 2E1 decay mode of the 2s metastable state) in the case of Ar ions and for $n \leq 5$ in the case of Kr. The detection efficiency has been carefully determined through dedicated experiments [11].

- The effect of transport processes on *fine structure components* of core excited states is determined using high-resolution high-transmission Bragg-crystal spectrometers equipped with mosaic graphite crystals (HOPG) and position sensitive detectors. Our crystal spectrometers are placed in a vertical geometry, allowing first order correction of the broadening of the emitted lines due to Doppler effect. A detailed description is presented in [12]. Additionally to the fine structure components, in the case of argon ions, we were able to record, with an extremely high resolution, the complete prompt Lyman series as shown in Figure 3.

Each detection system is placed at a specific angle with respect to the beam direction to be polarization-insensitive. Spectra recorded in the case of krypton ions are shown in [12] and [13].

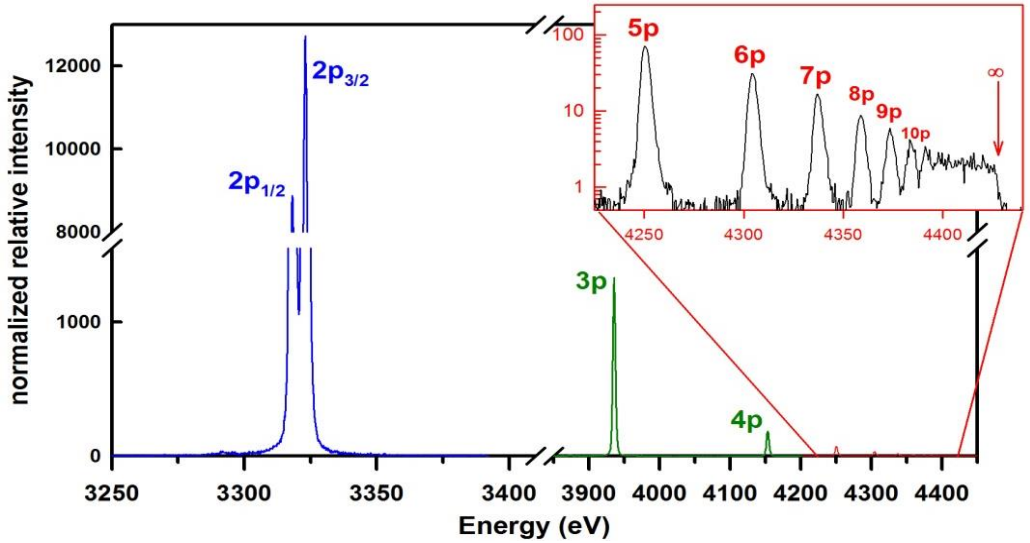

Figure 3. High resolution spectra of H-like X-ray transitions produced during the collision of Ar^{18+} ions at 13.6 MeV with a 47.2 µg/cm² (i.e. 220 nm) carbon target. All the np → 1s lines with $n \in [2, \infty]$ are recorded by accumulating data over different Bragg angle settings of the spectrometer. For the 2p level, the two components $2p_j$ with j = 1/2 and 3/2 are resolved. Note: the photon energy is given in the projectile frame.

3. Theoretical approaches

The ion-solid interaction represents a good example of a small open system in contact with a large reservoir. The open system is the internal state of a fast hydrogen-like ion while the reservoir consists of the radiation field and of the particles of the solid that induce energy exchange and decoherence in the small system. Hence, the starting point of any description of the ion-solid interaction is the reduced density operator $\sigma(t)$ whose time evolution follows the Liouville equation that includes dissipative and non-dissipative terms:

$$i\frac{\partial}{\partial t}\sigma(t) = [H_S, \sigma(t)] + R\sigma(t) \quad (1)$$

where H_S is the Hamiltonian of the small system which contains the Coulomb interaction potential possibly modified by the wake potential and R the relaxation operator describing its interaction with the reservoir.

We have suggested several theoretical simulations to solve equation (1) using different methods and various approximations. The coupling between the small open system and the reservoir is perturbative. Consequently, we show that the coupling element between two states due to the wake field is much smaller than the inverse of correlation times of vacuum fluctuations on one hand and of collisional processes on the other hand. It is then possible to use an extension of Bloch equations (see the work of C. Cohen-Tanoudji, J. Dupont-Roc and G. Grynberg [13]) or, in other words, a *master equations approach* (MEA) ([8, 11, 12]). This first approach consists of solving a set of differential coupled equations that allows following the evolution of populations of each $n\ell jm_j$ state and of coherences between states. In our approach, we neglect the damping of coherences through collisions. All the transition rates are calculated explicitly in the hydrogenic basis set used to describe the projectile electronic states. We account for all the cross sections of processes involved during transport (in fact, for collision, atomic cross sections of capture, ionization, intra-shell excitation with $\Delta\ell = \pm1$ and ±2 and inter-shell excitation with $\Delta n = \pm1$ and ±2 are included). In this treatment, the basis set consists of all the sub-states of the n = 1–6 shells. Actually, we found that convergence of calculations is reached around n = 6 (changes when going from n = 5 to 6 do not exceeds a few %). When neglecting the couplings between the off-diagonal matrix elements (the coherence effects) and the diagonal matrix elements of the reduced density matrix, the problem reduces simply to the resolution of differential equations giving the time evolution of only the excited $n\ell$ state populations referred to as *rate equations*. The *quantum transport theory* (QTT) initiated by the groups of J. Burgdörfer and C.O. Reinhold [9, 10, 14, 15] has been developed to overcome the problem of coherence transport and the limit in the number of states to be considered. The starting point of such a description is the possibility to write the relaxation operator R in equation (1) using the Lindblad approach [10, 16]. This insures the possibility to solve the quantum Liouville equation by means of a quantum trajectory Monte Carlo technique first used in quantum optics for the description of few-state atomic systems interacting with the radiation field (see for example the work of J. Dalibard *et al* [17]). In this approach, the reduced density operator $\sigma(t)$ of the system is constructed from the independent evolution of an ensemble of N_{traj} pure states. Each pure state evolution is called a quantum trajectory and describes a different random sequence of interactions with the environment through the non-linear stochastic Schrödinger equation. The QTT method can be considered as a quantized version of the corresponding *classical transport theory* (CTT) for which test particles (electron of the projectile ion) obey then the Langevin equation. This equation describes the motion of the electron on a classical orbit disturbed by a stochastic force [21-23]. This classical method does not take into account for the effects related to the spin of the electron and the radiative decay. As a result, the classical approximation will be only valid for Z_p ions not too heavy for which the spin-orbit coupling is rather weak and the radiative decay times long enough compared to the ion transit time inside the solid. These either deterministic or stochastic approaches have been compared between each other [9, 18] showing that the quantum MEA and QTT methods give similar results. What is interesting is the possibility to gauge the sensitivity of the experimental data to the transport effects by, for instance, switching “on/off” the influence of the wake field. Additionally, we may test the initial density matrix representing the primary process of population and notably the initial phase and extract an effective wake field value.

4. Results and discussions

One of our major contributions to the topics treated here is to have been able to confront theoretical approaches with experimental data on an absolute scale. Great cares have been taken to extract absolute experimental cross sections and, in parallel, efforts have been made to include in the theoretical developments all the ingredients so as to treat the complete dynamics of the interaction and therefore to reach a real understanding in the relevant parameters.

4.1. Rydberg state populations

An exhaustive experimental study of the production and transport of Rydberg excited states has been done for Ar^{18+} ions on solid carbon targets, at a velocity of 23 a.u., and for a range of thicknesses allowing us to span the transport conditions from single collision to equilibrium (3.5 to 201 µg/cm²). In this case, the number of collisions the projectile electron experiences in the solid is extensively varied from ~ 0.6 to 60 collisions in average. The evolution of the Lyα(*2p→1s*) and Lyβ(*3p→1s*) intensities as a function of the ion time of flight behind the thinnest and the thickest carbon foils used in the experiment is shown in Figure 4 (a series of results for the other target thicknesses are given in [8]). Keeping in mind that lifetimes of hydrogen-like nℓ states are proportional to $n^3\ell^2$ for a given projectile, the delayed photon emission observed in the decay of 2*p* and 3*p* states comes from the Rydberg state population through cascade contributions. The observed 2*p* decay time is much longer than the 3*p* one for all target thicknesses, which is indeed a direct signature of high angular momentum Rydberg states. With the CTT model, we demonstrate that the 2*p* state population, for this system, is sensitive to excited states up to n = 30 even though only 3% of the excited states have a principal quantum number $n > 10$. The comparison with the experimental data shows that the evolution of the population of highly excited states during the transport is mainly governed by multiple scattering (intra and inter-shell excitation processes). Indeed, the classical simulation with or without the wake field does not exhibit significant differences.

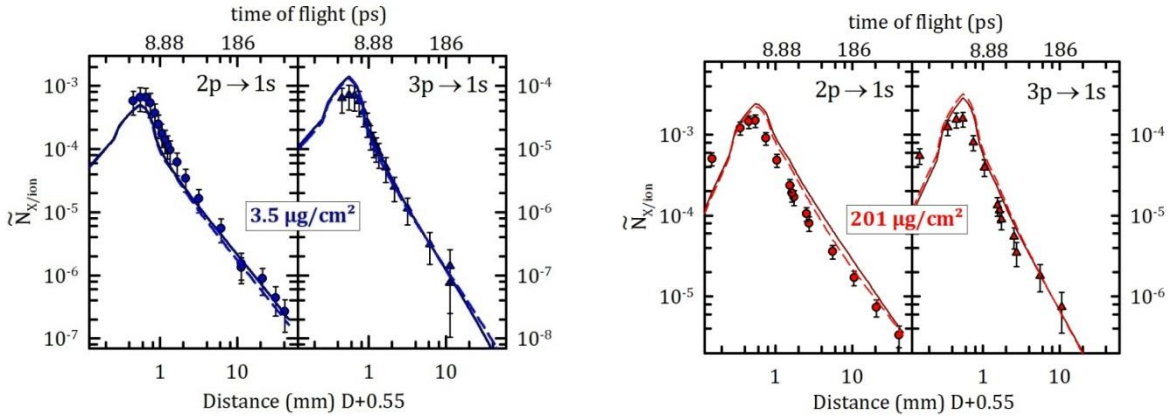

Figure 4. Evolution with the ion time of flight behind the target of the Ar^{17+} Lyman line intensities, i.e., number of emitted photons per ion, for the 3.5 and 201 µg/cm² carbon target [8]. Experimental results: symbols, CTT simulations with wake "off" (dashed lines) and wake "on" (solid lines). In the simulations, Continuum Distorted Wave (CDW) calculations have been used to account for the primary capture processes. The distance behind the target has been arbitrarily shifted by 0.55 mm for sake of clarity.

4.2. Core state populations

We illustrate in Figure 5 the evolution of absolute core *np* state populations as a function of target thickness, or alternatively as a function of ion transit time through solid foils for Kr^{35+} at 33.2 MeV/u and Ar^{17+} at 13.6 MeV/u. The dotted lines reported in Figure 5 that account only for binary ion-atom collisions i.e., without any transport effects, highlight clearly that the core *np* populations are sensitive to transport effects, especially, when increasing the principal quantum number. When comparing with the dashed lines, we observe that the major contribution in the evolution of the experimental data is due to collisional processes and radiative decay (note that in the case of argon only 3% of states

deexcite inside the solid). The sensitivity to the wake field is weak and appears more clearly in the case of argon mainly because the wake field scales roughly as $1/v_p^2$ with v_p the projectile velocity. Similar behaviors are observed for the evolution the *np* Lyman lines of Kr^{35+} at 60 MeV/u populated by the single 1s→2p excitation process as primary process [24]. In the case of argon, the 2s state population has also been examined and the great sensitivity to transport effects for the core state are shown in figure 6.

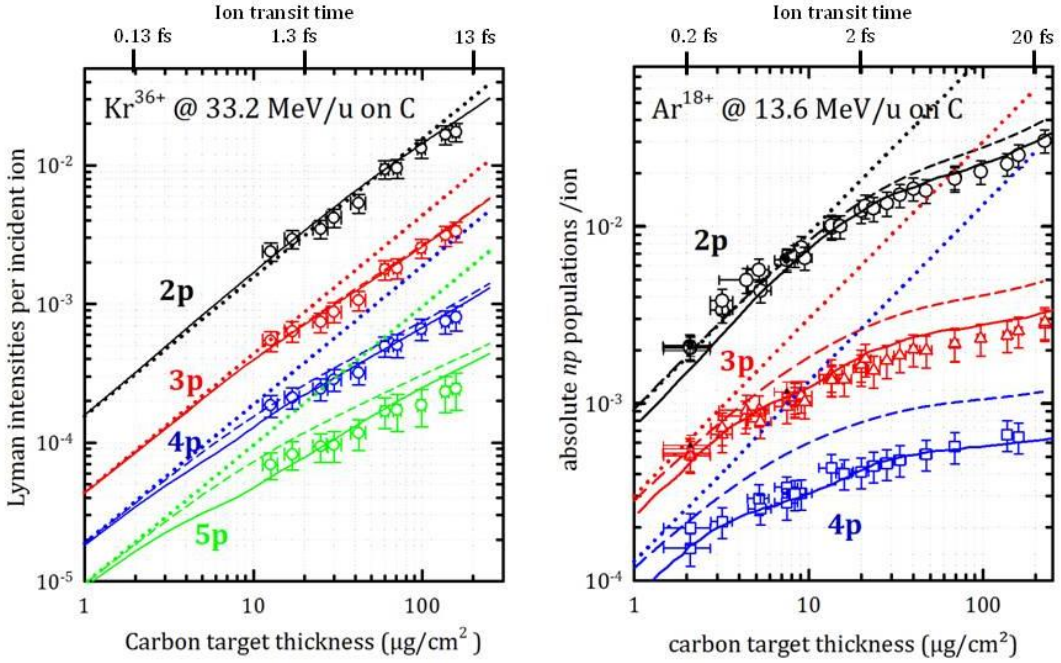

Figure 5. Absolute Lyman intensities (or populations) as a function of carbon target thickness (i.e., ion transit time) for two different collision systems. The dotted lines account only for binary ion-atom collisions (i.e., without any transport effects). The full and dashed lines correspond to the predictions of quantum approach (MEA for krypton and QTT for argon) with "wake on" and "wake off" respectively. In both cases, CDW calculations are used for the initial conditions of populations, i.e., the capture process.

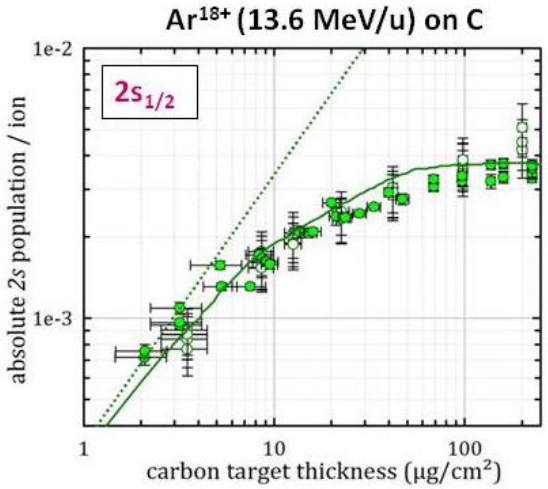

Figure 6. Evolution the 2s population as a function of the foil thickness. Symbols: experiment data. Dotted green line: results when no transport effects are included. Full green line: results predicted by QTT taking into account all the transport effects including the wake field [9].

4.3. Fine structure sub-state populations of core states

The observable exhibiting a strong sensitivity to the wake field is the evolution of the fine structure $n\ell j$ components, which is related to the Stark mixing and, consequently, to the coherence terms of the density matrix. More precisely, in order to gather quantitative evidence of the wake-field effect, we have investigated the relative populations of the fine structure components i) of the Balmer-α as the $3s_{1/2}$ / $3p_{1/2}$ and $3d_{3/2}$ / $3d_{5/2}$ s ratios in the case of krypton [13, 17, 19] and ii) of the Lyman-α as the $2p_{1/2}$ / $2p_{3/2}$ ratio in the case of argon [20].

In Figure 7, we present the case of H-like Kr ions initially populated by single excitation and transported through carbon foils. This collision system is very interesting in a sense that, in this case, the initial density matrix (the primary process) evaluated with Plane Wave Born Approximation calculations is well predicted. Hence, we test only the transport phase of our various theoretical approaches. With this figure, we better appreciate the sensitivity of the collisional effects, on one hand, and of the effect of the wake field, on the other hand. We note that the two quantum (MEA and QTT) approaches give similar results. For the $3p_{1/2}$ / $3s_{1/2}$ ratio, simulations with "wake off" (i.e., pure collisional approaches) predict first a decrease up to ~ 25 µg/cm² in clear contradiction with the observed experimental increase, which is, on the other hand, very well reproduced by the complete calculations that take into account the Stark coupling. This demonstrates that the wake field controls the evolution of hydrogen-like excited states. Moreover, the effective electric field deduced from the spatial extension of the wake field [7, 11] proves to be quite accurate. For the $3d_{3/2}$/$3d_{5/2}$ ratio that implies two states of the same $n\ell$ shell, collisional approaches predict, as expected, no evolution with the ion transit time. Taking into account the Stark mixing gives a good estimation of the asymptotic value. The ratio is slightly overestimated for intermediate thicknesses (~ 50-100 µg/cm²) but the disagreement is found to be around 10% at maximum.

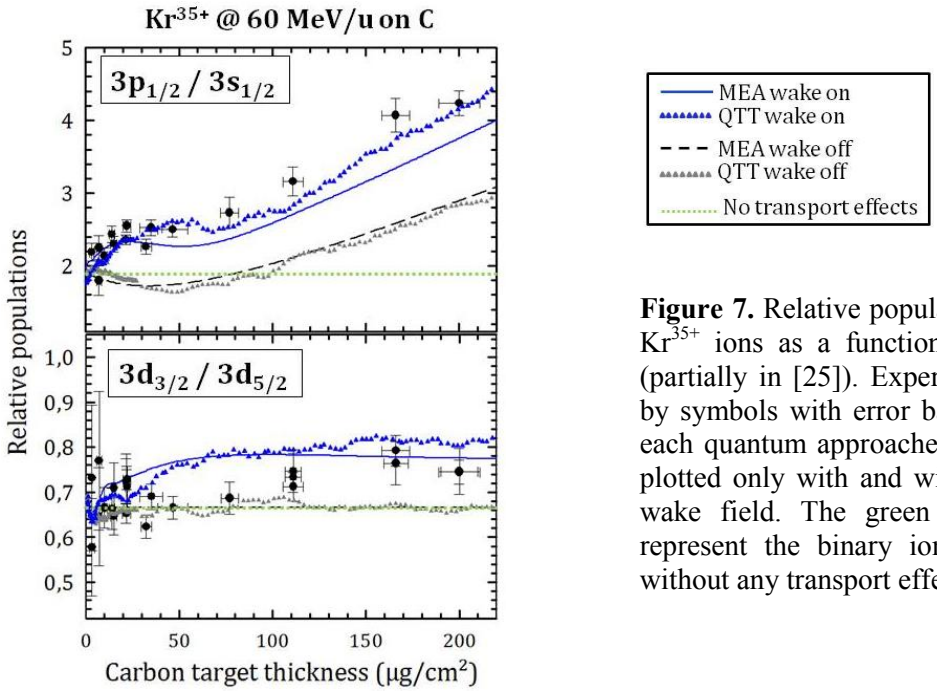

Figure 7. Relative population ratios in n = 3 for Kr^{35+} ions as a function of the foil thickness (partially in [25]). Experimental data are given by symbols with error bars. The predictions of each quantum approaches (MEA and QTT) are plotted only with and without the effect of the wake field. The green dashed straight lines represent the binary ion-atom collisions, i.e., without any transport effects.

For argon, the evolution of the $2p_{1/2}$ / $2p_{3/2}$ ratio is presented in Figure 8. As in the previous case, it varies significantly as a function of the target thickness. Here, when comparing the full predictions (black line) with those without Stark effect (dashed black line), we underline the major role of the wake field or, more precisely, the interplay between the wake field and the relativistic splitting of the energy level for this collision system. Changes as a function of ion penetration depth are well accounted for by our quantum transport simulation. Nevertheless, even if the general trend is satisfying, a clear discrepancy occurs at the "zero" thickness (i.e., the true single collision limit experimentally accessible with a gaseous target). For the primary process of charge transfer, the non relativistic calculations used here include only spin-independent interactions. As a result, the $n\ell j$

populations are linked to the nℓ populations through statistical factors leading to a ratio of 0.5. Experimentally, whatever the gas used (CH_4 or N_2), we found a value of 0.54 ± 0.01, ~ 10% larger than predicted indicating the presence of spin dependent relativistic corrections during the primary charge transfer even at a moderately relativistic speed. To estimate whether relativistic effects may explain the observed discrepancy, we have used the relativistic eikonal approximation to evaluate the ratio $2p_{1/2}$ / $2p_{3/2}$ [26]. A ratio of 0.52, at variance with 0.5, is predicted giving a hint that additional relativistic effects could be present. This ratio is nevertheless still insufficient to account for the experimental data. To have a better agreement for the thinner foils, a shift to a value of 0.56 is necessary (full blue line). Relativistic calculations of the one-electron capture density matrix at moderately relativistic velocities are missing to bring a final conclusion, the unprecedented accuracy of this type of measurements requiring thus new calculations.

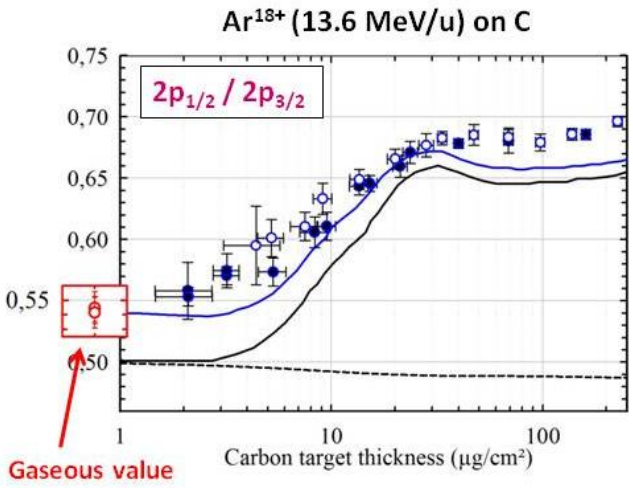

Figure 8. Lyman-α photon intensity ratio between $2p_{1/2} \rightarrow 1s$ and $2p_{3/2} \rightarrow 1s$ following transport of Ar^{17+} ions (initially Ar^{18+}) through carbon foils [26]. Symbols: experiment data. Note that the experimental value of the initial state (prior any transport) is shown (i.e., the gaseous value). Full black line: results predicted by QTT taking into account all the transport effects. Full blue line: as previous but with an adjusted ratio $R = \sigma_{2p1/2}/\sigma_{2p3/2}$. Dashed black line: predicted result when neglecting the wake field (equivalent to neglecting coherences).

5. Conclusions

The use of X-ray spectroscopy has allowed probing the ultra-fast dynamics of the ion-solid interaction as the X-ray emission is directly linked to the projectile ion excited state populations. The study of the evolution of high-ℓ Rydberg states as well as core nℓ and nℓ_j levels with the ion transit time inside the solid gives access to the response of the target electrons to the passage of the ion. The choice of collision partners (i.e., the projectile ion and the target whose thickness is varied) and of the collision velocity has allowed us to shed light on both features of the ion-solid interaction: the *collisional aspect* due to binary ion-atom processes (solid seen as an assembly of atoms) and the *collective response* via the wake field induced by the projectile. The theoretical description of the evolution of a small open system (the hydrogen-like projectile ion) in contact with a large reservoir (the solid) has been a great challenge. Whatever the approach used (Monte Carlo calculations or master equations), we succeeded to treat on the same footing all the competing processes occurring during the ion transport such as Stark mixing induced by the wake field following the projectile ion, elastic and inelastic collisions as well as radiative decay. The very good agreement between our experimental results and the simulations allow concluding that we have obtained a successful description of the ion transport in solid in the high velocity regime. In fact, it is remarkable to realize that our theoretical approaches first developed for dissipative processes in quantum optics implying a two- or three-level atom in interaction with an electromagnetic field may be generalized to a multi-level system in interaction with a reservoir including not only electromagnetic field but also collisions. In particular, we demonstrated that in ion-solid interaction, a collisional picture can be used to describe the high-ℓ Rydberg state

populations and the major part of $n\ell$ core state populations. For these observables, it is worthwhile to mention that a classical transport gives similar results to those obtained with a quantum approach provided the radiative decay during the transport is negligible. Regarding in more details the $n\ell$ states and above all the relative $n\ell_j$ sub-state populations, we have shown that a pure collisional approach completely fails to reproduce their evolution inside the solid. Actually, the evolution of the relative fine-structure populations with the target thickness is well predicted provided Stark couplings induced by the wake field is accounted for. In more details, when the initial conditions are well known as, for instance, in the case of Kr^{35+} at 47 a.u. populated by single excitation in carbon, we found that the value of the wake field extracted from ion stopping power measurements is also correct to reproduce our experimental results. In other words, our experiment can be considered as the first direct measurement of the wake field. To go beyond, the sensitivity of our observable is such that we can also test the initial conditions (i.e., the initial density matrix) as seen in the case of Ar^{17+} at 23 a.u. populated by capture in carbon. For this collision system, a complete calculation on a $n\ell_j$ basis including relativistic effects is still needed to evaluate the one-electron capture density matrix proving, in particular, that the initial coherences in the capture process even at moderately relativistic velocities are not well theoretically described.

References

[1] Bethe H 1930 *Ann. Phys.* **5** 325
[2] Olivera G, Martinez A, Rivarola R and Fainstein P 1994 *Phys. Rev.* A **49** 603
[3] Schiwietz G, Wille U, Díez Muiño R, Fainstein R and Grande P 1996 *J. Phys.* B **29** 307
[4] Bohr N 1948 *K. Dansk. Vidensk. Selsk. Mat. Fys. Medd.* **18** 1
[5] Neufeld J and Ritchie R 1955 *Phys. Rev.* **98** 1632
[6] Echenique P, Flores F and Ritchie R 1990 Solid State Physics **43**, New York Academic 229: Ehrenreich H and Turnbull D
[7] Fuhr J, Ponce V, Garcia de Abajo F and Echenique P 1998 *Phys. Rev.* B **57** 9329
[8] Lamour E, Gervais B, Rozet J-P and Vernhet D 2006 *Phys. Rev.* A **73** 042715
[9] Seliger M, Reinhold C, Minami T, Schultz D, Pindzola M, Yoshida S, Burgdörfer J, Lamour E, Rozet J-P and Vernhet D 2007 *Phys. Rev.* A **75** 032714
[10] Minami T, Reinhold C and Burgdörfer J 2003 *Phys. Rev.* A **67** 022902
[11] Rozet J-P, Vernhet D, Bailly-Despiney I, Fourment C and Dubé L 1999 *J. Phys.* B **32** 4677
[12] Fourment C 2000 PhD thesis Université Pierre et Marie Curie
[13] Vernhet D, Rozet J-P, Bailly-Despiney I, Stephan C, Cassimi A, Grandin J-P and Dubé L 1998 *J. Phys.* B **31** 117
[14] Lamour E, Prigent C, Eberhardt B, Rozet J-P and Vernhet D 2009 *Rev. Sci. Instrum.* **80** 023103
[15] Adoui L 1995 PhD thesis Université Pierre et Marie Curie
[16] Cohen-Tanoudji C, Dupont-Roc J and Grynberg G 1988 *Processus d'interaction entre photons et atomes* Inter Editions/Editions du CNRS
[17] Reinhold C, Seliger M, Minami T, Yoshida S, Burgdörfer J, Mestayer J, Zhao W, Lancaster J and Dunning F 2007 *J. Phys. Conf. Series* **88** 012030
[18] Seliger M 2005 PhD thesis Technishe Universität Wien
[19] Lindblad G 1976 *Com. Math. Phys.* **48** 119
[20] Dalibard J, Castin Y and Molmer K 1992 *Phys. Rev. Lett* **68** 580
[21] Gervais B, Reinhold C and Burgdörfer J 1996 *Phys. Rev.* A **53** 3189
[22] Lamour E 1997 PhD thesis Université de Caen Basse Bormandie
[23] Reinhold C, Arbo D, Burgdörfer J, Gervais B, Lamour E, Vernhet D and Rozet J-P 2000 *J. Phys.* B **33** L111
[24] Vernhet D, Fourment C, Lamour E, Rozet J-P, Gervais B, Dubé L, Martin F, Minami T, Reinhold C, Seliger M and Burgdörfer J 2001 *Phys. Scr.* **T92** 233
[25] Reinhold C, Seliger M, Minami T, Schultz D, Burgdörfer J, Lamour E, Rozet J-P and Vernhet D 2007 *Nucl. Instrum. Meth.* B **261** 125
[26] Seliger M, Reinhold C, Minami T, Schultz D, Yoshida S, Burgdörfer J, Lamour E, Rozet J-P and Vernhet D 2008 *Phys. Rev.* A **77** 042713